A R C H I V E S O F M E T A L L U R G Y A N D M A T E R I A L S
Volume 49 2004 Issue 2

B.B. STRAUMAL *

GRAIN BOUNDARY PHASE TRANSITIONS. INFLUENCE ON DIFFUSION, PLASTICITY AND CHARGE TRANSFER

PRZEJŚCIA FAZOWE NA GRANICACH ZIAREN I ICH WPŁYW NA DYFUZJĘ, PLASTYCZNOŚĆ ORAZ TRANSFER ŁADUNKU

Increased diffusion permeability of polycrystals (especially that of nanograined ones) in many cases can be attributed to the grain boundary (GB) phase transitions. They influence also liquid-phase and activated sintering, soldering, processing of semi-solid materials. The GB wetting phase transition can occur in the two-phase area of the bulk phase diagram where the liquid (L) and solid (S) phases are in equlibrium. The GB wetting tieline appears in the $L+S$ area. Above the temperature of the GB wetting phase transition a GB cannot exist in equlibrium contact with the liquid phase. The liquid phase has to substitute the GB and to separate both grains. The GB wetting tie-line can continue in the one-phase area of the bulk phase diagram as a GB solidus line. This line represents the GB premelting or prewetting phase transitions. The GB properties change drastically when GB solidus line is crossed by a change in the temperature or concentration. In case if two solid phases are in equilibrium, the GB "solid state wetting" (or covering) can occur. In this case the layer of the solid phase *2* has to substitute GBs in the solid phase *1*. Such covering GB phase transition occurs if the energy of two interphase boundaries between phase *1* and *2* is lower than the GB energy in the phase *1*.

Lepsza dyfuzyjność polikryształów (zwłaszcza tych o wielkości ziarna w skali nanometrycznej) często związana jest z tzw. przejściami fazowymi granic ziaren. Przejścia fazowe na granicach ziaren wywierają również istotny wpływ na spiekanie z udziałem fazy ciekłej, spajanie materiałów oraz inne procesy w stanie pół-stałym. Przykładowo zjawisko zwilżania granic ziaren zachodzi w obszarze dwufazowym na wykresie fazowym, gdzie faza ciekła *(L)* i stała *(S)* są w stanie równowagi. Konsekwencją jest istnienie dodatkowych linii zwilżalności w obszarze $L+S$, które określają temperaturę przejścia fazowego zwanego zwilżaniem granic ziaren. Powyżej tej temperatury granica ziarna nie jest w stanie równowagi z fazą ciekłą i przechodzi w stan ciekły, pomimo że ziarna, które rozdziela są w stanie stałym. Linie zwilżania granic ziaren mogą występować także w obszarze jednofazowym wykresu fazowego. Wtedy charakteryzują temperatury innych przejść fazowych granic ziaren definiowanych jako nadtopienie oraz przedzwilżanie. Właściwości granic ziaren ulegają znacznym zmianom w sytuacji, gdy linia solidus dla

* INSTITUTE OF SOLID STATE PHYSICS, CHERNOGOLOVKA, MOSCOW DISTR. 142432 RUSSIA

granicy ziarna krzyżuje się ze zmianą temperatury lub stężenia. Gdy dwie fazy są w stanie równowagi, obserwuje się tzw. zwilżanie w stanie stałym (lub zestalanie). Wtedy warstwa fazy stałej 2 zastępuje granice ziaren w fazie stałej 1.

1. Introduction

The properties of modern materials, especially those of nanocrystalline, superplastic or composite materials, depend critically on the properties of internal interfaces such as grain boundaries (GBs) and interphase boundaries (IBs). All processes which can change the properties of GBs and IBs affect drastically the behaviour of polycrystalline metals and ceramics [1]. GB phase transitions are one of the important examples of such processes [2]. Recently, the lines of GB phase transitions began to appear in the traditional bulk phase diagrams [2–7]. The addition of these equilibrium lines to the bulk phase diagrams ensures an adequate description of polycrystalline materials, particularly their diffusion permeability, deformation behavior and the evolution of the microstructure. In this work the following GB phase transitions are discussed: (a) GB wetting, (b) GB prewetting (or premelting) and (c) GB «wetting» (covering) by second solid phase. The recently obtained experimental data are discussed. Using these data, the new GB lines in the conventional bulk phase diagrams are constructed.

2. Grain boundary wetting phase transitions

In this work GB wetting, prewetting and premelting phase transitions are considered. The GB melting, GB faceting transition and the "special GB – random GB phase transitions" are analyzed elsewhere [8–10]. One of the most important GB phase transitions is the *GB wetting transition*. Since their prediction by Cahn [11] the study of wetting phase transitions has been of great experimental and theoretical interest, primarily for planar solid substrates and fluid mixtures [12–14]. Particularly, it was experimentally shown that the wetting transition is of first order, namely the discontinuity of the surface energy was measured and the hysteresis of the wetting behavior was observed [15, 16]. The important difference is that in case of GB wetting only two phases coexist, namely the liquid (melt) phase and the solid one containing the boundary between the misoriented grains. Therefore, the contact angle θ also depends only on two different surface energies (the GB energy σ_{GB} and the energy of the solid/liquid interphase boundary σ_{SL}) instead of three ones in the usual experiments: $\sigma_{GB} = 2\sigma_{SL} \cos(\theta/2)$. If $\sigma_{GB} < 2\sigma_{SL}$, the GB is incompletely wetted and the contact angle $\theta > 0$ (Fig. 1a). At the temperature T_W of the GB *wetting phase transition* $\sigma_{GB} = 2\sigma_{SL}$ and at $T \geq T_W$ the GB is completely wetted by the liquid phase and $\theta = 0$ (Fig. 1b). If two GBs have different energies the temperatures of their GB wetting transitions will also differ: the lower σ_{GB}, the higher T_W (Figs. 1c and 1d). If the GB wetting phase transition is of first order, there is a discontinuity in the temperature derivative of the GB energy at T_W

which is equal to $[\partial\sigma_{GB}/\partial T - \partial(2\sigma_{SL})/\partial T]$ [11, 16]. If the GB wetting phase transition is of second order, $\partial\sigma_{GB}/\partial T = \partial(2\sigma_{SL})/\partial T$ at T_W. The theory predicts also the shape of the temperature dependence θ (T) at $T \rightarrow T_W$: it must be convex for a first order wetting transition [$\theta \sim \tau^{1/2}$ where $\tau = (T_W - T)/T_W$] and concave for a second order wetting transition: $\theta \sim \tau^{3/2}$ [12]. Our preliminary results demonstrate that the GB phase transitions of the second order may occur in Zn GBs wetted by the Al-rich melt. The $\theta(T)$ dependence is concave in this system and the discontinuity in the temperature derivative of the GB energy at T_W is negligibly small. In polycrystals the whole spectrum of GBs exists with various energies. Therefore, in polycrystals the maximal T_{wmax} and minimal T_{wmin} can be found for high-angle GBs with minimal and maximal energy σ_{GBmin} and σ_{GBmax}, respectively (Fig. 2).

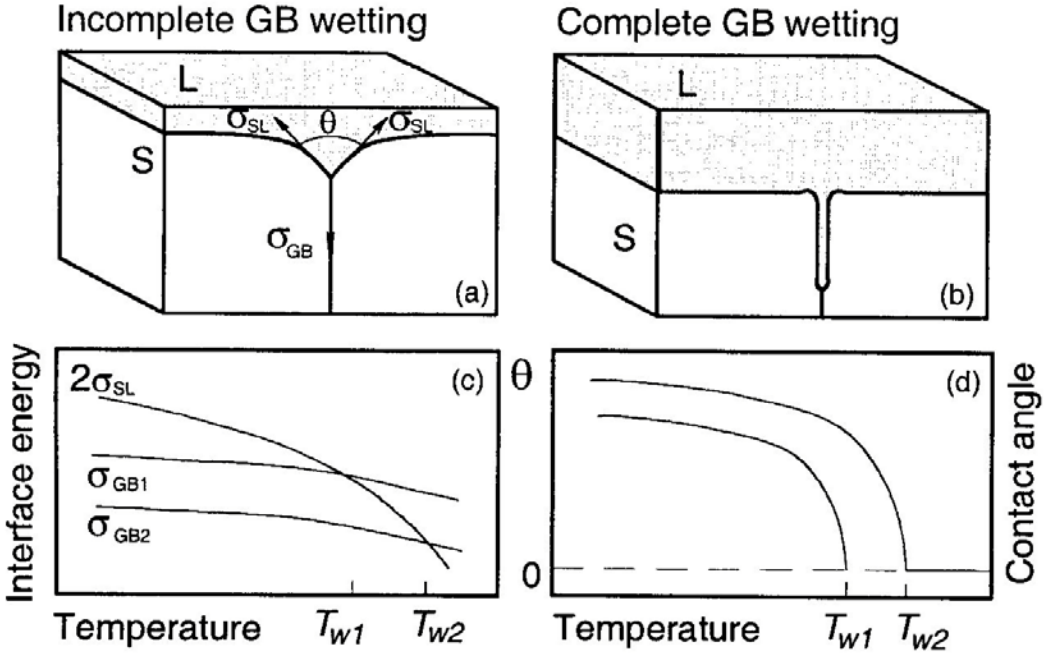

Fig. 1. (a) Scheme of the equilibrium contact between the grain boundary in the aolid phase S and the liquid phase L (incomplete wetting). (b) Complete GB wetting. (c) Sheme of the temperature dependence for the GB energy σ_{GB} (for two different GBs) and the energy of the solid-liquid interface boundary σ_{SL}. (d) Scheme of the temperature dependence of the contact angle θ for two grain boundaries with energies σ_{GB1} and σ_{GB2}. T_{W1} and T_{W2} are the temperatures of the GB wetting phase transition

First indications of the GB wetting phase transitions were found by measuring of the contact angles in polycrystals [17]. Correct measurements were later perfomed using metallic bicrystals with inndividual tilt GBs in the Al–Sn, Cu–In [4], Al–Pb–Sn [3,18,19], Al–Ga, Al–Sn–Ga [20, 21], Cu–Bi [5, 22, 23, 30], Fe–Si–Zn [24–27], Mo–Ni [28], W–Ni [29] and Zn–Sn [7] systems. The tie-lines of the GB wetting phase transition were constructed basing on the experimental data [3, 4, 7, 18–29]. The difference in the GB wetting phase transition temperature was experimentally revealed for GBs with different energies [4, 18]. The indications of presence of the liquid-like phase along the dislocation lines were also found [23].

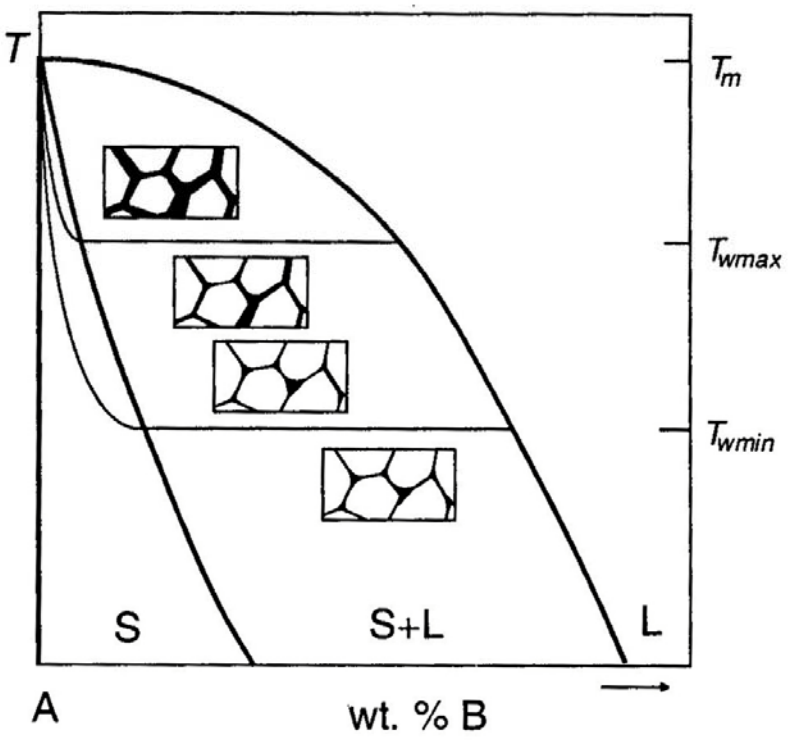

Fig. 2. Scheme of the phase diagram with lines of bulk and GB phase transition. Thick lines represent the bulk phase transitions. Thin lines represent the tie-lines of the GB wetting phase transition in the $S + L$ area for the high angle GBs having maximal and minimal possible energy and the GB premelting phase transition in the solid solution area S

The deformation behavior of metals in the semi solid state has been extensively investigated from the viewpoint of rheological flow [30–32]. These studies have shown that the viscosity of the semi-solid metals depends on the volume fraction and morphology of the solid phase and the shear strain rate. In addition, the deformation behavior in a semi-solid state at the early stages of melting has been investigated by compressive creep tests [33–36]. V a a n d r a g e r and P h a r r [24] showed that the deformation mechanism in a semi-solid state at the early stages of melting is grain boundary sliding accommodated by cavitation in a liquid phase for the copper containing a liquid bismuth. This deformation mechanism in the semi-solid state at the early stages of melting appears to be different from that in the semi-solid state during solidification. The presence of a liquid phase gives rise to complicated effects on the deformation behavior in the semi-solid state. Deformation in the semi-solid state is phenomenologically divided as follows: plastic deformation of solid phases, sliding between solid phases, flow of liquid incorporating solid phases and liquid flow [22]. For compressive deformation, because the liquid phase is squeezed out of boundaries experiencing compressive stresses in a very short time [24], it is difficult to investigate deformation related to the liquid flow by compressive tests. In [37] the shear tests were carried out over a wide temperature range of 480–620°C, including temperatures below and above the solidus temperature, for Al – 5 wt.% Mg alloy to investigate deformation behavior in semi-solid states at early stages of melting. P h a r r et al. [36] showed that the liquid phase significantly affects creep behavior of alloys when a significant portion of the grain boundary area, in excess of 70%, is wet. This revealed that

the volume fraction of the liquid phase is an important factor in the deformation characteristics in the semi-solid state. The same trend has been reported in a semi-solid state at solidification [34]. However, deformation in the semi-solid state is very complicated and cannot be characterized only by the volume fraction of a liquid phase. In [37] the pure shear of Al – 5 wt% Mg alloy was investigated. This method permits to exclude the squeezing of the liquid phase from the sample. The shear strain to failure drops drastically at the solidus temperature (Fig. 3) [37]. In the semi-solid phase it is about 6 times lower than in the solid solution. Using the micrographs of the structure of polycrystals in the semi-solid state from [37] we calculated the fraction of the fully wetted GBs in dependence on the temperature. The continuous increase of the fraction of wetted GBs with increasing temperature influences strongly the mechanism of the deformation. In Fig. 4 the temperature dependence of the shear strain rate is shown recalculated from the data [37]. In the solid solution the shear strain rate increases moderately with increasing temperature, and the activation energy (135 kJ/mol) is very close to the activation energy of Mg diffusion in Al (131 kJ/mol). In the semi-solid state the shear strain rate increases drastically. Close to T_{wmax} the (formally calculated) activation energy is about 1650 kJ/mol, i.e. ten times higher than the activation energy for the viscosity of Al melt. It means that in the semi-solid state no unique thermally activated mechanism is working. Due to the temperature increase of the fraction of wetted GBs, the structure of the solid skeleton changes continuously. It becomes more and more cutted with increasing temperature, therefore, making the shear easier in addition to the pure temperature activation.

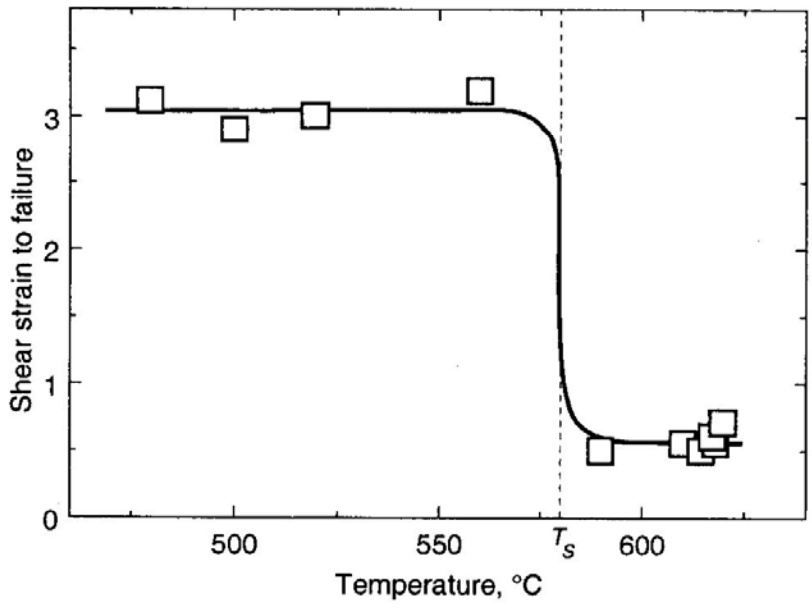

Fig. 3. Temperature dependence of shear strain to failure for Al–5 wt. % Mg alloy in solid and semi-solid state [37]

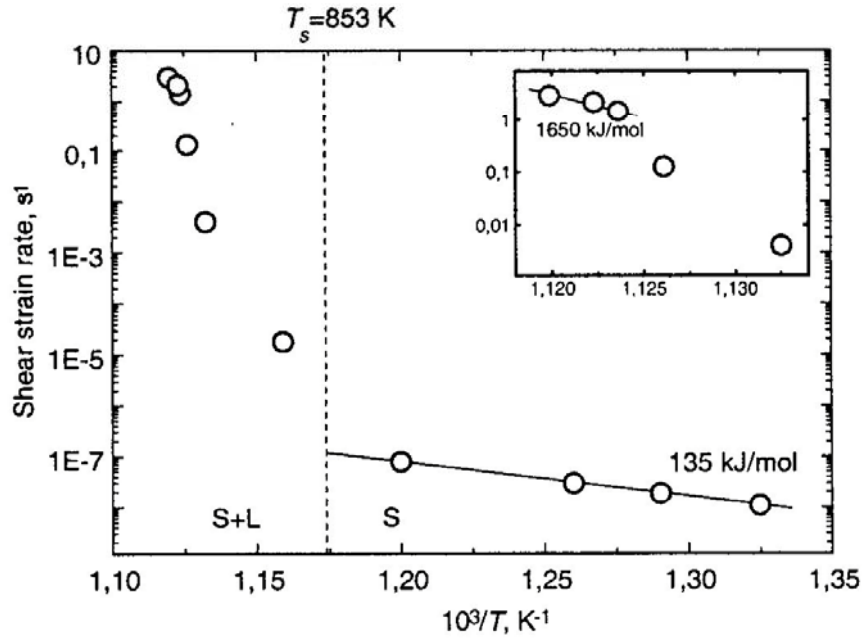

Fig. 4. Temperature dependence of shear strain rate for Al–5 wt. % Mg alloy in solid and semi-solid state [37]

3. Grain boundary prewetting (Premelting) phase transitions

It was pointed out by Cahn [38] that, when the critical consolution point of two phases is approached, GBs of one critical phase should be wetted by a layer of another critical phase, and in the one-phase region of a phase diagram there should be a singularity connected with an abrupt transition to a microscopic wetting layer. We distinguish two possible situations: the first one, when a layer of the new phase is formed on the GB (*prewetting transition*), and the second one, when the GB is replaced by a layer of the new phase (*premelting phase transition*). At the prewetting transition the difference between two phases must be small, while at the premelting transition the wetting phase may differ from that of the bulk dramatically. The lines of the GB prewetting or premelting phase transitions appear in the one-phase areas of the bulk phase diagrams where only one bulk phase can exist in the thermodynamic equilibrium (e.g. solid solution S, see Fig. 2). These lines continue the tie-lines of the GB wetting phase transitions and represent the GB solidus (Fig. 2). The thin liquid-like layer of the GB phase exists on the GBs between the bulk solidus and GB solidus in the phase diagram. During the GB premelting phase transition this layer appears abruptly on the GB by the intersection of GB solidus. As a result, the GB properties (diffusivity, mobility, segregation) change dramatically.

In other words, above the GB wetting tieline T_W in the $S + L$ area of the bulk phase diagram $\sigma_{GB} > 2\sigma_{SL}$. This is true also if we intersect the bulk solidus at $T =$ const and move into the one-phase area S of the bulk phase diagram. The GB energy σ_{GB} in this part of the one-phase region is still higher that the energy $2\sigma_{SL}$ of two solid-liquid interphase boundaries. Therefore, the GB still can be substituted by two solid-liquid interfaces, and the energy gain $\Delta G = \sigma_{GB} - 2\sigma_{SL}$ appears by this substitution. G permits to stabilize the GB

layer of the liquid-like phase. The appearance of the liquid-like phase (otherwise unstable in the bulk) between two *S/L* interfaces instead of GB leads to the energy loss Δg per unit thickness and unit square. Therefore, the GB layer of the liquid-like phase has the thickness l defined by the equation $\sigma_{GB} - 2\sigma_{SL} = \Delta g l$. Thickness l depends on the concentration and temperature and becomes $l = 0$ at the line of GB premelting (or prewetting) phase transition.

The premelting transition has been revealed in the ternary Fe–Si–Zn system by measurements of Zn GB *diffusivity* along tilt GBs in the Fe–Si alloys [24–27]. It was found that the penetration profiles of Zn along GBs consist of two sections, one with a small slope (high GB diffusivity $D_b\delta$) at high Zn concentrations and one with a large slope (low GB diffusivity) at low Zn concentrations (Fig. 5). The transition from one type of behavior to the other was found to occur at a definite Zn concentration c_{bt} at the GB, which is an equilibrium characteristic of a GB and depends on the temperature and pressure. The GB diffusivity increases about two orders of magnitude which is an indication of a quasi-liquid layer present in the GBs at high Zn concentration. The line of GB premelting phase transition in the one-phase area of the bulk phase diagram continues the line of the GB wetting phase transion in the two-phase $L + S$ area: by pressure increase both the GB wetting and the GB enhanced diffusivity disappear together at the same pressure value [27].

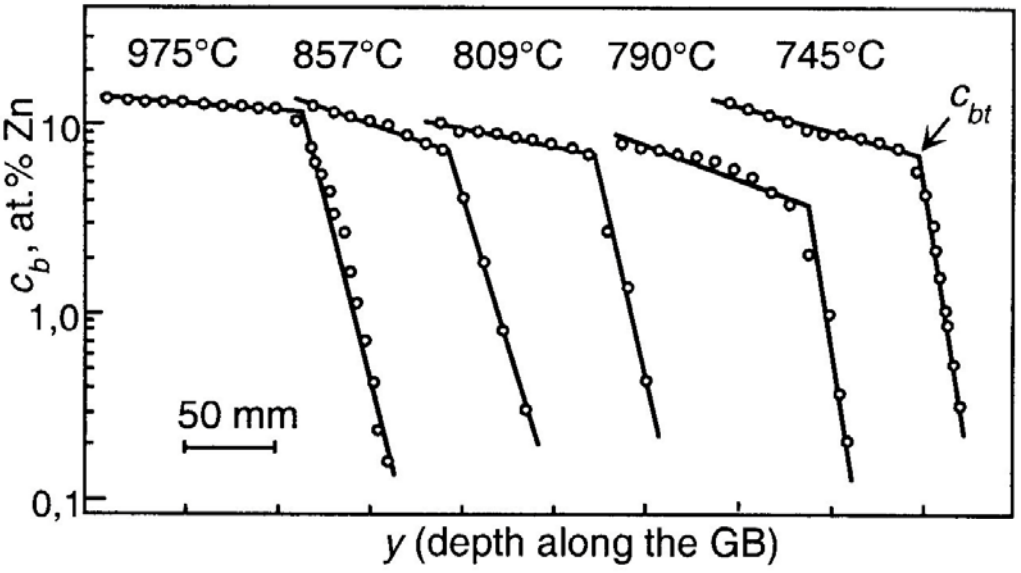

Fig. 5. Dependences of the GB Zn concentration c_b after diffusion into the GBs in Fe–5 at. Si bicrystals on the depth y in Fisher's coordinates $1g\, c_b - y$ at various temperatures [24]. All these curves possess the high-$D_b\delta$ part (with low slope) and low- $D_b\delta$ part (with high slope). The $D_b\delta$ changes abruptly at their intersection c_{bt}

The *GB mobility* was studied for two tilt GBs in bicrystals grown of high purity 99.999 wt.% Al and of the same material doped by 50 wt. ppm Ga [21]. The GB mobility increased about 10 times by addition of the Ga content for the both GBs studied. Normally, the addition of a second component can only decrease the GB mobility due to the solution drag [32]. The increase of the GB mobility can only be explained by the formation of the liquid-like Ga-rich layer on the GBs as a result of a premelting phase transition. The *GB segregation* of Bi in Cu was studied in the broad temperature and concentration interval [5,

22, 23, 39, 40]. It was shown that at a fixed Bi concentration the GB segregation Z_Φ changes abruptly at a certain temperature. Below this temperature the GB Bi concentration is constant and corresponds to a thin layer of pure Bi (GB phase). Above this temperature the GB segregation is lower than one monolayer of Bi and decreases gradually with increasing temperature according to the usual laws. These features indicate also the formation of a thin layer of a GB phase in the one-phase area of the bulk Cu–Bi phase diagram. The points of the abrupt change of the GB segregation form the GB solidus line in the bulk Cu–Bi phase diagram [22, 23, 39, 40]. GB segregation was measured with the aid of Auger electron spectroscopy (AES) on the GB fracture surfaces in samples broken *in situ* in the AES instrument. In other words, the multilayer GB segregation in Cu–Bi alloys leads to the increased *GB brittleness*. In [41] the GB energy was measured in Cu–Bi alloys using individual $\Sigma 19$ GB in bicrystals with the aid of the GB thermal grooves. The thermal groove profile was obtained with the aid of atomic force microscopy. The GB Bi segregation was measured simultaneously in the same conditions. The abrupt change of the segregation coincides with the *discontinuity of GB energy*. This fact demonstrates that the GB premelting (or prewetting) phase transition is of first order. The low-temperature measurements of resistivity temperature coefficient $d\rho/dT$ and residual resistivity ρ_0 at 4 K were performed in [40] using the Cu–Bi polycrystals annealed at high temperature and subsequently quenched. Both $d\rho/dT$ and ρ_0 demonstrate well pronounced break exactly at the same position where the sudden change of GB segregation was observed. In other words, the formation of GB layers of liquid-like phase leads to the measurable changes of *resistivity*.

The enhanced diffusion in case of existence of liquid-like GB phase can improve the plasticity of materials. For examplee, the superplastic forming of micrograined and nanostructured materials is a commercial, viable, manufacturing technology. One of the major drawbacks of conventional superplastic forming is that the phenomenon is only found at relatively low strain rates, typically about 10^{-4} to 10^{-3} s^{-1}. Recently, a number of studies have indicated that superplasticity of nanostructured materials can sometimes occur at extremely high strain rates (greater than 10^{-3} s^{-1} and up to 10^{2} s^{-1}). A specific example is a tensile elongation of over 1250% recorded at a strain rate of 10^{2} s^{-1} [42]. Thus far, this phenomenon, denoted as high-strain-rate superplasticity (HSRS), has been reported in several classes of materials, including metal alloys [42], metal-matrix composites [43–46] and mechanically-alloyed materials [47–49]. Despite these extensive experimental observations, the fundamental understanding of the factors leading to HSRS has not yet been arrived at. One very pertinent fact is that all of the materials that exhibit HSRS have a very fine grain size (~ 1 μm and less). Another is that the phenomenon is observed at rather high homologous matrix temperatures and very close to the matrix solidus temperature. In Fig. 7 the example is shown of HSRS for the 7475 Al–Zn–Mg alloy. The data are taken from independent works [50, 51] and reveal the very good reproducibility of the effect. Both temperature dependences have rather narrow maximum few degrees below the solidus temperature T_S. It is important to mention that the soludus temperature was measured by the differential thermal analysis (DTA) in the same works [50, 51]. The maximum elongation to failure reaches 1250 %. Below T_S the maximal elongation is about 500 %, above T_S the maximal elongation drops very quickly down to almost 0%.

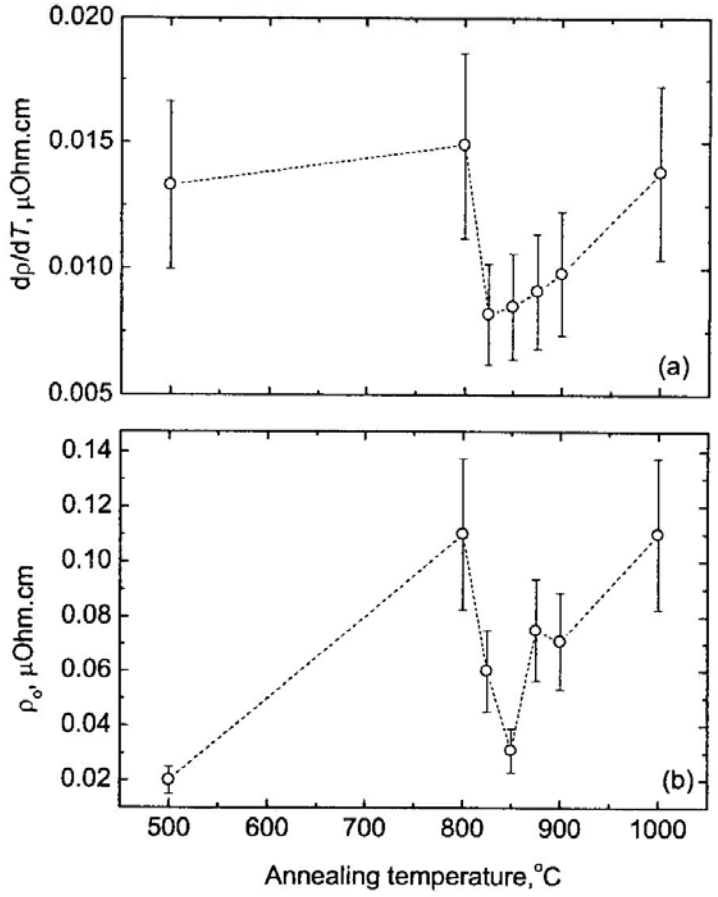

Fig. 6. (a) Dependence of the temperature derivative of the resistivity $d\rho/dT$ and (b) residual resistivity ρ_o of the Cu – 75 at. ppm Bi polycrystals on the annealing temperature

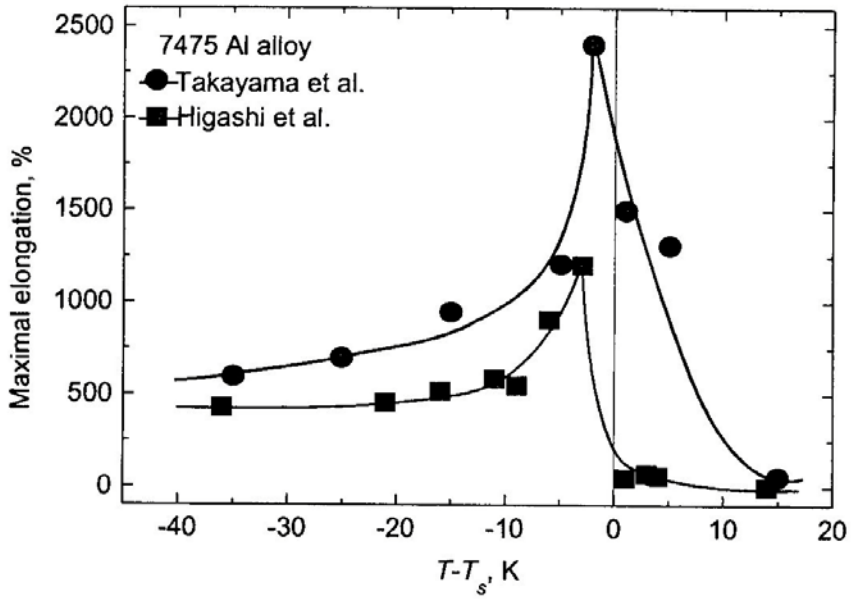

Fig. 7. The temperature dependence of the maximal elongation of the 7475 Al–Zn–Mg alloy samples. T_S is the solidus temperature. Circles represent the data [50] and squares are taken from [51]

We suppose that the HSRS phenomenon can be explained using the ideas on the GB phase transitions in the two-phase $S + L$ area and the solid solution area of the bulk phase diagrams. Using the data published in the literature, we constructed the lines of the GB wetting phase transition for the 7xxx Al–Zn–Mg alloys (Fig. 8). The liquidis line has been constructed using the linear interpolation of liquidus lines for the binary Al–Mg and Al–Zn phase diagrams [52]. Solidus has been drawn through the melting point for Al [52] and experimental points obtained using DTA for the 7xxx alloys and transition from solid to semi-solid mechanical behavior [35, 50, 51, 53]. The analysis of the microstructures published in [35, 50, 51] permitted us to estimate the fraction of completely and partially wetted GBs. These estimations allow to construct the GB wetting transition tie-lines (thin solid lines) for the T_{wmax} (above T_{wmax} all high-angle GBs in the polycrystal are completely wetted) [50, 51] and $T_{w50\%}$ (above $T_{w50\%}$ about 50% of the high-angle GBs in the polycrystal are completely wetted) [35]. The experimental points represent the data of mechanical tests [50, 53–55]. Full squares mark the maximal elongation-to-failure obtained in the tests performed at different temperatures [50, 51, 54]. They lie either below the bulk solidus line or coincide with it. The temperature difference between temperature of the maximal elongation-to-failure and T_s decreases with increasing concentration of Mg and Zn. According to the thermodynamics, the tielines of the GB wetting phase transition cannot finish at the intersection with the bulk solidus. They have to form the GB solidus line which continue in the solid solution area of the bulk phase diagram and finish in the melting point of the pure component. In the limiting case the degenerated GB solidus coincide with the bulk solidus. But in some systems it can extend into the solid solution area like it is shown in Fig. 4. In that case the layer of the liquid-like GB phase exist in the GBs between the GB and bulk solidus lines. We have shown above that the presence of such liquid-like layer in GB leads to the enhanced GB diffusivity, mobility and segregation of the second component [5, 11–17]. Such GB solidus lines are drawn also in Fig. 9 (thin solid lines). They continue the T_{wmax} and $T_{w50\%}$ GB wetting tie lines and finish in the melting point of Al. The GB solidus lines are drawn in such a way that the points of the maximal elongation-to-failure are between the GB and bulk solidus. Therefore, the enhanced plasticity of the nanograined polycrystals can be explained by the GB phase transition leading to the formation of the liquid-like layer on the GB in the narrow band of the solid solution area, just below the bulk solidus line. The phase diagrams similar to those shown in Fig. 8 can be constructed using the published data on HSRS, DTA and microscopy also for the 2xxx (Al–Zn–Mg) [45, 47–59, 51, 56–58], 5xxx (Al–Mg) [47, 51, 59, 60] and 6xxx (Al–Si–Mg) [59, 61–64] alloys. All authors studied the HSRS phenomenon mention that the physical reason of such a huge and reproducible increase of the palsticity is unknown. We suppose, therefore, that the HSRS phenomenon can be explained by the existence of the equilibrium GB liquid-like layer close to the bulk solidus.

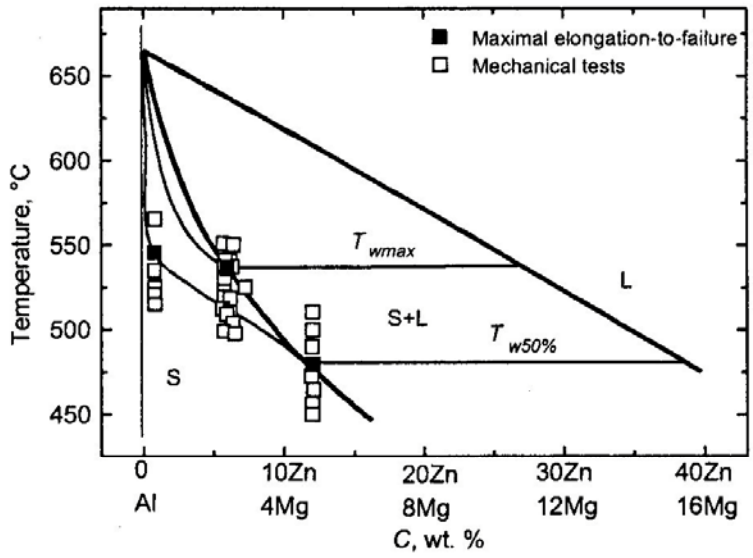

Fig. 8. The phase diagram containing the GB wetting phase transition tie-lines and GB solidus lines constructed for the 7xxx Al–Zn–Mg alloys

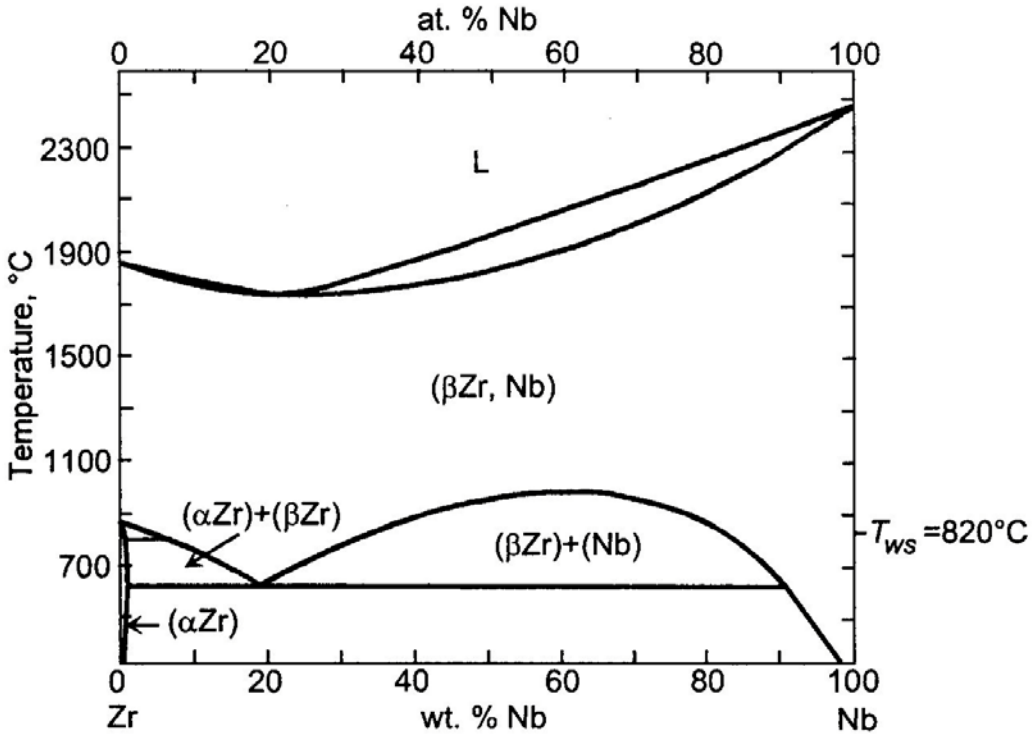

Fig. 9. Phase diagram Zr–Nb with lines of the bulk phase transitions (thick solid lines) and the tie-line of the GB covering phase transition at 820°C (thin solid line)

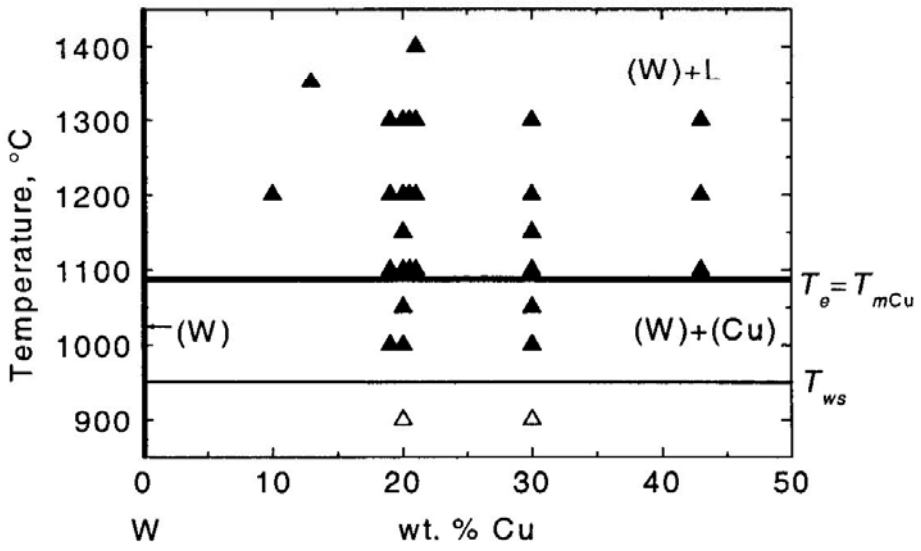

Fig. 10. Phase diagram W–Cu with lines of the bulk phase transitions (thick solid lines) and the tie-line of the GB covering phase transition at 950°C (thin solid line). The experimental points correspond to the two different GB morphologies in the W–Cu polycrystals [66–71]. Solid triangles: GBs in W are wetted by the layers of liquid (Cu) phase or covered by the solid (Cu) phase. Open triangles: GBs in W are not covered by the solid (Cu) phase

4. Grain boundary wetting (Covering) by solid phase

The situation illustrated in Fig. 1 can repeat in case if second phase (β) is not liquid but also solid. In other words, if in the phase α the GB energy $\sigma_{\alpha\alpha}$ is lower that the energy of two α/β solid/solid interfaces, the GB α/α has to be substituted by the layer of the second solid phase β. Such process can be called the GB wetting (or covering) by solid phase. It is clear, that the kinetics of the equlibration processes in case GB wetting (or covering) by solid phase is much slower than in case of wetting by liquid phase. Another examples of the GB covering phase transitions can be found by the analysis of the data published in the literature. In Fig. 9 the phase diagram Zr–Nb is shown. Thick solid lines represent the bulk phase transitions. The thin solid line represents the tie-line of the GB covering phase transition at 820°C. Above this line the high-temperature (β-Zr, Nb) phase forms the continuous thick layers in the α-Zr GBs [65]. In Fig. 10 the W–Cu phase diagram is shown with lines of the bulk phase transitions (thick lines) and the tie-line of the GB covering phase transition at 950°C (thin line). The experimental points correspond to the two different GB morphologies in the W–Cu polycrystals obtained by liquid phase sintering or activated sintering [66–71]. Solid triangles correspond to the GBs in W which are wetted by the layers of liquid (Cu) phase or covered by the solid (Cu) phase. Open triangles denote the GBs in W which are not covered by the solid (Cu) phase.

5. Conclusions

The GB phase transitions can be observed both in two-phase and one-phase areas of the conventional phase diagrams for the bulk phase transitions. In the two-phase $S+L$ area

where solid and liquid phases are in equilibrium the GB wetting phase transition can take place at T_w. Above T_w the GB disappears being substituted by two solid/liquid interfaces and the (macroscopically thick) layer of the liquid phase. The tie-lines of the GB wetting phase transition must have a continuation (GB solidus) in the one-phase S area of the bulk phase diagram. By intersection of GB solidus line the GB prewetting or premelting phase transition proceeds. Between the lines of GB and bulk solidus the grain boundary is substituted by two solid/liquid interfaces and the thin layer of the liquid-like phase. This liquid-like phase is stable in the GB and unstable in the bulk. The liquid-like phase is stabilized in GB due to the energy gain which appears as a result of substitution of GB by two solid/liquid interfaces. The GB wetting and prewetting (premelting) phase transitions observed up-to-date are of first order. If the GB energy is higher than the energy of two solid/solid interfaces, the GB solid state wetting (covering) phase transition can occur in a two-phase $S_1 + S_2$ area of the phase diagram.

Acknowledgements

The financial support of Russian Foundation for Basic Research RFBR Copernicus program of EU (contract ICA2-CT-2001-10008), INTAS grant 03-51-3779 and the German Federal Ministry for Education and Research is acknowledged.

REFERENCES

[1] T.G. Langdon, T. Watanabe, J. Wadsworth, M.J. Mayo, S.R. Nutt, M.E. Kassner, Mater. Sci. Eng. A **166**, 237-242 (1993).
[2] B.B. Straumal, W. Gust, Mater. Sci. Forum, **207-209**, 59-68 (1996).
[3] B. Straumal, D. Molodov, W. Gust, J. Phase Equilibria, **15**, 386-391 (1994).
[4] B. Straumal, T. Muschik, W. Gust, B. Predel, Acta metall. mater. **40**, 939-945 (1992).
[5] L.-S. Chang, E. Rabkin, B.B. Straumal, S. Hofmann, B. Baretzky, W. Gust, Defect Diff. Forum, **156**, 135-146 (1998).
[6] B. Straumal, V. Semenov, V. Glebovsky, W. Gust, Defect Diff. Forum, **143-147**, 1517-1522 (1997).
[7] B.B. Straumal, W. Gust, T. Watanabe, Mater. Sci. Forum, **294-296**, 411-414 (1999).
[8] F. Ernst, M.W. Finnis, A. Koch, C. Schmidt, B. Straumal, W. Gust, Z. Metallk. **87**, 911-922 (1996).
[9] B.B. Straumal, L.S. Shvindlerman, Acta metall. **33**, 1735-1749 (1985).
[10] E.L. Maksimova, L.S. Shvindlerman, B.B. Straumal, Acta metall. **36**, 1573-1583 (1988).
[11] J.W. Cahn, J. Chem. Phys. **66**, 3667-3679 (1977).
[12] S. Dietrich, Wetting transitions in interfaces, in C. Domb and J.H. Lebowitz (eds.), Phase Transitions and Critical Phenomena, **12**, 2-218, Academic Press, London (1988).
[13] D. Jasnov, Rep. Prog. Phys. **47**, 1059-1070 (1984).
[14] G. de Gennes, Rev. Mod. Phys. **57**, 827-863 (1985).
[15] H. Kellay, D. Bonn, J. Meunier, Phys. Rev. Lett. **71**, 2607-2610 (1993).
[16] J.W. Schmidt, M.R. Moldover, J. Chem. Phys. **79**, 379-387 (1983).
[17] N. Eustathopoulos, L. Coudurier, J.C. Joud, P. Desre, J. Crystal Growth **33**, 105-115 (1976).
[18] B. Straumal, W. Gust, D. Molodov, Interface Sci. **3**, 127-132 (1995).

[19] B. Straumal, D. Molodov, W. Gust, Mater. Sci. Forum **207-209**, 437-440 (1996).
[20] B. Straumal, S. Risser, V. Sursaeva, B. Chenal, W. Gust, J. Physique IV 5-C7, 233-241 (1995).
[21] D.A. Molodov, U. Czubayko, G. Gottstein, L.S. Shvindlerman, B.B. Straumal, W. Gust, Phil. Mag. Lett. **72**, 361-368 (1995).
[22] L.-S. Chang, B.B. Straumal, E. Rabkin, W. Gust, F. Sommer, J. Phase Equilibria 18, 128-135 (1997).
[23] L.-S. Chang, E. Rabkin, B. Straumal, P. Lejcek, S. Hofmann, W. Gust, Scripta mater. **37**, 729-735 (1997).
[24] E.I. Rabkin, V.N. Semenov, L.S. Shvindlerman, B.B. Straumal, Acta metall. mater. **39**, 627-639 (1991).
[25] O.I. Noskovich, E.I. Rabkin, V.N. Semenov, L.S. Shvindlerman, B.B. Straumal, Acta metal. mater. **39**, 3091-3098 (1991).
[26] B.B. Straumal, O.I. Noskovich, V.N. Semenov, L.S. Shvindlerman, W. Gust, B. Predel, Acta metall. mater. **40**, 795-801 (1992).
[27] B. Straumal, E. Rabkin, W. Lojkowski, W. Gust, L.S. Shvindlerman, Acta mater. **45**, 1931-1940 (1997).
[28] E. Rabkin, D. Weygand, B. Straumal, V. Semenov, W. Gust, Y. Brechet, Phil. Mag. Lett. **73**, 187-193 (1996).
[29] V.G. Glebovsky, B.B. Straumal, V.N. Semenov, V.G. Sursaeva, W. Gust, High Temp. Mater. Proc. **13**, 67-73 (1994).
[30] M.C. Flemings, Metall. Trans. **A 22**, 957-981 (1991).
[31] P. Kumar, C.L. Martin, S. Brown, Metall. Trans. **A 24**, 1107-1116 (1993).
[32] C.P. Chen, C.-Y.A. Tsao, Acta mater. **45**, 1955-1968 (1997).
[33] M.C. Roth, G.C. Weatherly, W.A. Miller, Acta metall. **28**, 841-853 (1980).
[34] B.L. Vaandrager, G.M. Pharr, Acta metall. **37**, 1057-1066 (1989).
[35] B. Baudelet, M.C. Dang, F. Bordeaux, Scripta Metall. Mater. **32**, 707-712 (1995).
[36] H. Iwasaki, T. Mori, M. Mabuchi, K. Higashi, Acta mater. **46**, 6351-6360 (1998).
[37] G.M. Pharr, P.S. Godavarti, B.L. Vaandrager, J. Mater. Sci. **24**, 784-792 (1989).
[38] J.W. Cahn, J. Phys.Colloq. **43-C6**, 199-213 (1982).
[39] L.-S. Chang, E. Rabkin, B.B. Straumal, B. Baretzky, W. Gust, Acta mater. **47**, 4041-4046 (1999).
[40] B. Straumal, N.E. Sluchanko, W. Gust, Def. Diff. Forum **188-190**, 185-194 (2001).
[41] J. Schölhammer, B. Baretzky, W. Gust, E. Mittemeijer, B. Straumal, Interf. Sci. **9**, 43-53 (2001).
[42] K. Higashi, S. Tanimura, T. Ito, MRS Proc. **196**, 385-390 (1990).
[43] T. Imai, M. Mabuchi, Y. Tozawa, M. Yamada, J. Mater. Sci. Lett. **2**, 255-257 (1990).
[44] M. Mabuchi, T. Imai, J. Mater. Sci. Lett. **9**, 761-762 (1990).
[45] T.G. Nieh, C.A. Henshall, J. Wadsworth, Scripta Metall. **18**, 1405-1408 (1984).
[46] M. Mabuchi, K. Higashi, Y. Okada, S. Tanimura, T. Imai, K. Kubo, Scripta Metall. **25**, 2003-2008 (1991).
[47] T.G. Nieh, P.S. Gilman, J. Wadsworth, Scripta Metall. **19**, 1375-1378 (1985).
[48] T.R. Bieler, T.G. Nieh, J. Wadsworth, A.K. Mukherjee, Scripta Metall. **22**, 81-86 (1988).
[49] K. Higashi, Y. Okada, T. Mukai, S. Tanimura, Scripta Metall. **25**, 2053-2057 (1991).
[50] Y. Takayama, T. Tozawa, H. Kato, Acta mater. **47**, 1263-1270 (1999).
[51] K. Higashi, T.G. Nieh, M. Mabuchi, J. Wadsworth, Scripta metall. mater. **32**, 1079-1084 (1995).
[52] I. Apykhtina, B. Bokstein, A. Khusnutdinova, A. Peteline, S. Rakov, Def. Diff. Forum, **194-199**, 1331-1336 (2001).
[53] T. Imai, M. Mabuchi, Y. Tozawa, Y. Murase, J. Kusul, in R.B. Bhagat. et al. (eds.), Metal & Ceramic Matrix Composites: Processing, Modeling & Mechanical Behavior 235-239, TMS-AIME, Warrendale, Pennsylvania (1990).

[54] M. Mabuchi, K. Higashi, T. Imai, K. Kubo, Scripta Metall. **25**, 1675-1680 (1991).
[55] N. Furushiro, S. Hori, Y. Miyake, in S. Hori et al., (eds.) Proc. Int. Conf. Superplast. Adv. Mats (ICSAM-91) 557-562, Jap. Soc. Res. Superplast., Tokyo (1991).
[56] M. Mabuchi, K. Higashi, T. Langdon, Acta metall. mater. **42**, 1739-1745 (1994).
[57] M. Mabuchi, K. Higashi, S. Wada, S. Tanimura, Scripta Metall. **26**, 1269-1274 (1992).
[58] T.G. Nieh, J. Wadsworth, Scripta Metall. **28**, 1119-1124 (1993).
[59] M. Mabuchi, K. Higashi, K. Inoue, S. Tanimura, Scripta Metall. **26**, 1839-1844 (1992).
[60] J. Koike, M. Mabuchi, K. Higashi, Acta metall. mater. **43**, 199-206 (1995).
[61] M. Mabuchi, K. Higashi, Y. Okada, S. Tanimura, T. Imai, K. Kubo, Scripta Metall. **25**, 2517-2522 (1991).
[62] T. Hikosaka, T. Imai, T.G. Nieh, J. Wadsworth, Scripta Metall. **31**, 118-11186 (1994).
[63] R.B. Grishaber, R.S. Mishra, A.K. Mukherjee, Mat. Sci. & Eng. **A 220**, 78-84 (1996).
[64] T.G. Nieh, D.R. Lesuer, C.K. Syn, Scripta Metall. Mater. **32**, 707-712 (1995).
[65] M.J. Iribarren, O.E. Agüero, F. Dyment, Def. Diff. Forum. **194-199**, 1211-1216 (2001).
[66] Ya.E. Geguzin, Physics of Sintering, 2nd edition. Nauka, Moscow (1984) (in Russian).
[67] V.N. Eremenko, Yu.V. Naidich, I.A. Lavrinenko, Sintering in the Presence of Liquid Phase, Naukova dumka, Kiev (1968) (in Russian).
[68] V.V. Panichkina, M.M. Sirotjuk, V.V. Skorokhod, Poroshk. Metall. **6**, 21-24 (1982) (in Russian).
[69] V.V. Skorokhod, V.V. Panichkina, N.K. Prokushev, Poroshk. Metall. **8**, 14-19 (1986) (in Russian).
[70] V.V. Skorokhod, Yu.M. Solonin, N.I. Filippov, A.N. Poshin, Poroshk. Metall. **9**, 9-14 (1983) (in Russian).
[71] W.J. Huppmann, H. Riegger, Acta metall. **23**, 965-971 (1975).

Received: 1 March 2004.